

**This is a self-archived version of an original article. This version may differ from the original in pagination and typographic details.**

**Author(s):** Maxwell, Lindley; Martínez, Héctor; Martín-Rodríguez, Alejandro; Gómez-Coca, Silvia; Rissanen, Kari; Ruiz, Eliseo

**Title:** Metal–Organic Nanocapsules with Functionalized s-Heptazine Ligands

**Year:** 2021

**Version:** Accepted version (Final draft)

**Copyright:** © 2020 American Chemical Society

**Rights:** In Copyright

**Rights url:** <http://rightsstatements.org/page/InC/1.0/?language=en>

**Please cite the original version:**

Maxwell, L., Martínez, H., Martín-Rodríguez, A., Gómez-Coca, S., Rissanen, K., & Ruiz, E. (2021). Metal–Organic Nanocapsules with Functionalized s-Heptazine Ligands. *Inorganic Chemistry*, 60(2), 570-573. <https://doi.org/10.1021/acs.inorgchem.0c03631>

# Metal-Organic Nanocapsules with Functionalized s-Heptazine Ligands

Lindley Maxwell,<sup>a</sup> Héctor Martínez,<sup>a</sup> Alejandro Martín-Rodríguez,<sup>a</sup> Silvia Gómez-Coca,<sup>a</sup>  
Kari Rissanen,<sup>b\*</sup> Eliseo Ruiz<sup>a\*</sup>

<sup>a</sup>Departament de Química Inorgànica and Institut de Recerca de Química Teòrica i Computacional, Universitat de Barcelona, Diagonal 645, 08028 Barcelona, Spain.

<sup>b</sup>University of Jyvaskyla, Department of Chemistry, Nanoscience Center P.O. Box 35, 40014 University of Jyvaskyla, Finland

## ABSTRACT

A metallo-organic capsule was synthesized where the ligand is a derivative of heptazine with three carboxylic groups which are coordinated to Cu<sup>II</sup> cations forming paddle-wheels motifs. Each nanocapsule is neutral with twelve Cu<sup>II</sup> centers and eight ligands adopting a rhombicuboctahedron shape. It has almost 3 nm diameter and the main intermolecular interactions in the solid are  $\pi \cdots \pi$  stackings between the C<sub>6</sub>N<sub>7</sub> heptazine moieties. The nanocapsules can form monolayers deposited on graphite characterized by atomic force microscopy, by confirming their stability in solution.

Studies of rational synthesis of discrete metal-organic nanocapsules with specific shapes and structures have been extensively carried out by several research groups.<sup>1-5, 6, 7-14</sup> An additional feature to the self-assembly process in the synthetic process is to provide to these nanocapsules additional chemical and physical properties. In this case, we have employed as ligand a heptazine derivative synthesized from polymeric derivatives of s-heptazine,<sup>15</sup> also known as graphitic carbon nitride (g-C<sub>3</sub>N<sub>4</sub>), which has been recently proposed for many catalytic processes (see Fig.1).<sup>16-19</sup> One of the main problems working with heptazine derivatives is their low solubility. The goal of this manuscript is to show that it is possible to overcome the solubility problems and synthesize nanocapsules with the C<sub>6</sub>N<sub>7</sub> moieties. In addition, this approach shows that the larger size of the heptazine ligands opens the possibility to generate nanocapsules while the equivalent s-triazine system (see Fig.1) results in periodic metal-organic frameworks (see Fig. S5).<sup>20</sup>

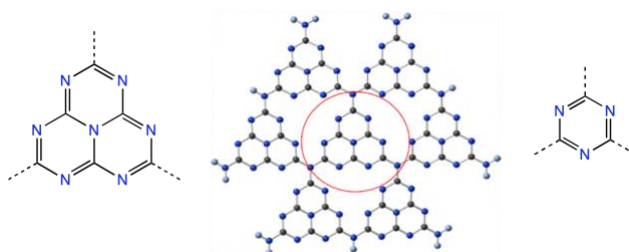


**Figure 1.** (left) s-heptazine, (center) g-C<sub>3</sub>N<sub>4</sub> and (right) s-triazine.

The goal was to form a nanocapsule using a 4-connected paddle-wheel subunits [M<sub>2</sub>(-COO)<sub>4</sub>] as vertex, where the carboxylic binding groups belongs to a tritopic heptazine derivative ligand. The synthesis of this ligand involves several steps (Fig. 2, see SI for reaction details).<sup>21</sup> First, the pyrolysis of urea at high temperature to obtain the polymeric [C<sub>6</sub>N<sub>7</sub>(NH)(NH<sub>2</sub>)]<sub>n</sub> *melon 1*, depending of the thermal treatment we can also reach the dehydrogenated system, g-C<sub>3</sub>N<sub>4</sub>. The second step is an alkali hydrolysis to synthesize the trialkoxide derivative **2** through a solid-

state reaction with  $\text{PCl}_5$  to obtain the trichloro derivative **3** (cyameluric chloride). Finally, the substitution reaction with 4-piperidinecarboxylic acid (4pac, also called isonipecotic acid) results in the ligand **4**. It is microwave assisted reaction that uses  $\text{NaHCO}_3$  as base and 1,4 dioxane as solvent.

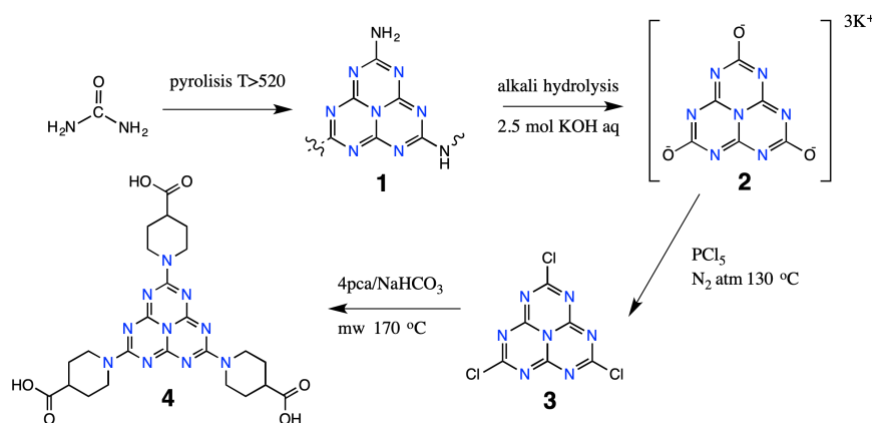


**Figure 2.** Synthesis of the ligand **4**, 1,1',1''-(1,3,3a<sup>1</sup>,4,6,7,9-heptaazaphenalene-2,5,8-triyl)tris(piperidine-4-carboxylic acid (h3tp4c, mw: microwave, see Table S2 for infrared characterization).

The relative low-solubility of **4** difficults the reaction with the metal (see Table S1 for the results of multiple attempts, also including cases with  $\text{Zn}^{\text{II}}$  cations) but the reaction with  $\text{Cu}(\text{NO}_3)_2 \cdot 3\text{H}_2\text{O}$  in DMSO in a sealed vial at  $110^\circ\text{C}$  results in the  $\text{Cu}_{12}$  nanocapsule **5** (see Fig. 3). The similar reaction with an equivalent triazine ligand and  $\text{Zn}^{\text{II}}$  cations results in a periodic structure<sup>20</sup> with a metal/ligand ratio of 12/4. In that case on each paddle-wheel structure, two of the carboxylic group ligands are coordinated to the same moiety but the other two are coordinated to a different unit (see Fig. S5). However, the relatively large size of the heptazine derivate ligand allow to form a nanocapsule with 12  $\text{Cu}^{\text{II}}$  cations and 8 heptazine ligands resulting in a neutral system. The structure of **5** can be describe as a rhombicuboctahedron (se

Fig. S6) where the six Cu<sub>2</sub> paddlewheel subunits (including the piperidine moiety) form the six edges of the cube and the heptazine moieties constitute the eight triangular faces.

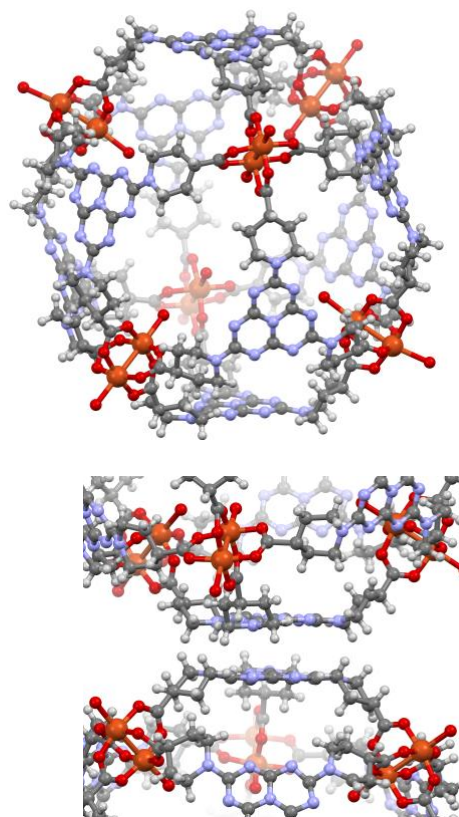


**Figure 3.** (above) Structure of complex **5** [Cu<sub>12</sub>(tp4c)<sub>8</sub>(H<sub>2</sub>O)<sub>12</sub>]. Orange, blue, grey and red ellipsoids correspond to copper, nitrogen, carbon and oxygen atoms, respectively. (below) Structure detail of the intermolecular  $\pi$ - $\pi$  stacking through the heptazine groups between two neighbour Cu<sub>12</sub> nanocapsules.

The charge-neutral nanocapsule **5** packs (see Fig. 3 bottom and Fig. S7) through the  $\pi$ - $\pi$  interactions with an interplanar distance of 3.5 Å between the C<sub>6</sub>N<sub>7</sub> heptazine units of the nanocapsules. The diameter of the nanocapsule is ca. 3 nm with 2.5 nm distance between the outer paddle-wheel Cu-atoms. The nanocapsule has an internal cavity of 2600 Å<sup>3</sup> (see cavity details Fig. S8), but due to the moderate resolution of the diffraction data none of the DMSO solvent molecules could not be located inside the cavity. The nanocapsule is not completely

closed as there are ten ellipsoidal windows, ca. 0.7 nm in diameter, allowing the small solvent molecules to “swim” through the cavity in solution.

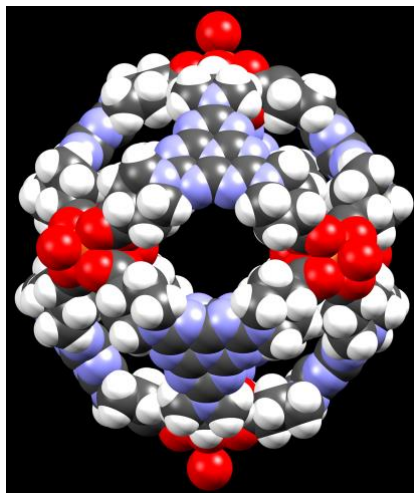


**Figure 4.** The space-filling model presentation of the structure of complex **5**  $[\text{Cu}_{12}(\text{tp4c})_8(\text{H}_2\text{O})_{12}]$  showing the shape of the 0.7 nm windows.

In order to complete the structural characterization, we have employed a 1:100 dilution of the mother liquor to deposit a monolayer of the complex **5** on highly oriented pyrolytic graphite (immersion time 30 s). The sample was abundantly cleaned with DMSO in order to eliminate the molecules that were not attached to the substrate through  $\pi$ - $\pi$  interactions. The sample was measured using an atomic force microscope (AFM) (see details in SI, section 5). We performed a scratch with the microscope tip of the monolayer to determine the thickness of the monolayer (see Figure 5) cleaning the substrate surface. The thickness value around 2.2 nm is in agreement with the size of the molecule (the molecule is slightly larger almost 3 nm in direction of two outer paddle-wheel groups) assuming that one of the heptazine groups is interacting with the graphite surface. This fact confirms the stability of complex **5** in solution despite its large size.

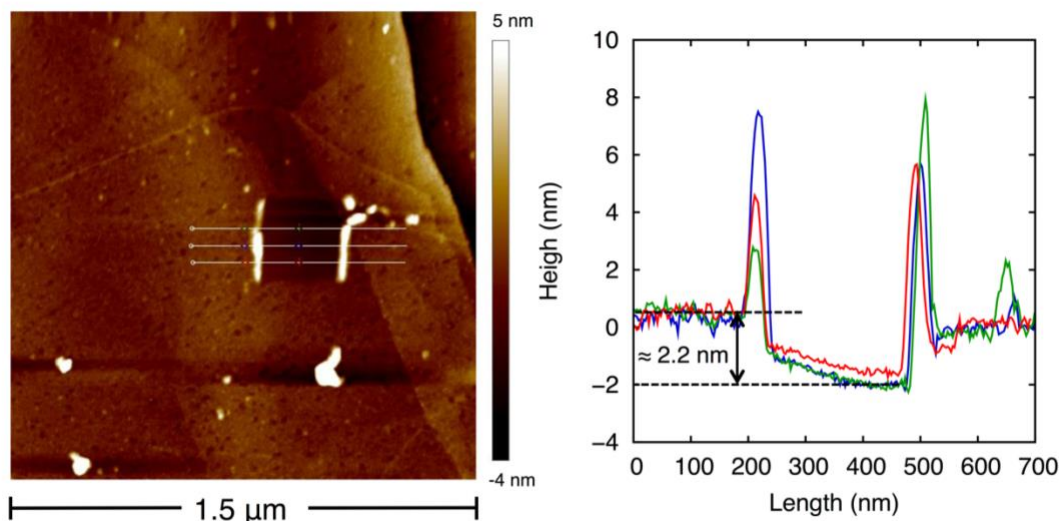


**Figure 5.** (left) AFM image of the monolayer of **5** deposited on HOPG. (right) The cross-section profiles in the tip scratched area at the position indicated by the lines in the AFM image.

The photochemical properties of ligand **4** (see Figs. 6 and S9) and dodecanuclear complex **5** (see Fig. S10) have been explored. From these data, we can outline some points: (i) the heptazine-based ligand **4** has a high absorbance with an extinction coefficient of  $1.1 \cdot 10^5 \text{ M}^{-1} \text{ cm}^{-1}$ , while the value for the complex is one order of magnitude smaller  $1.8 \cdot 10^4 \text{ M}^{-1} \text{ cm}^{-1}$ ; (ii) ligand **4** has a large Stokes shift of 110 nm (absorption 273 nm and emission 383 nm, see Fig. 5) indicating a large structural rearrangement of the molecule in the excited state. These structural variations should lead to a new conformation in the lower-energy excited state that might be the responsible of the red-shift in the emission maxima. The quantum yield of the ligand **4** determined by using an integrating sphere is 3.8%. (ii) The quenching effects in the  $[\text{Cu}_{12}(\text{tp4c})_8(\text{H}_2\text{O})_{12}]$  are important and the system does not present fluorescence (see UV-vis spectra, Fig. S10). It is worth noting that a previously reported  $\text{Cu}_3$  complex<sup>21</sup> with pyridyl-heptazine ligands shows fluorescence because the  $\text{Cu}^{\text{II}}$   $d_{x^2-y^2}$  orbitals are orthogonal to the  $\pi$  system of the heptazine moieties, however, that is not the case in **5** (see Fig. S11).

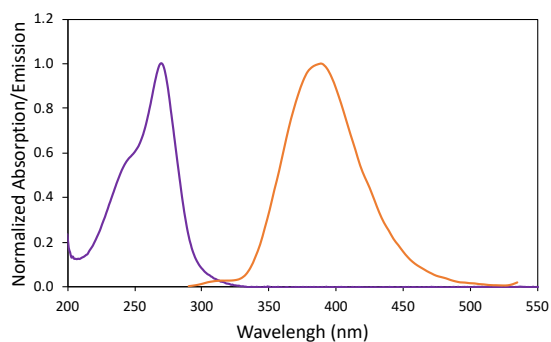


**Figure 6.** Absorption (purple) and emission (orange) spectra of ligand **4** at  $10^{-6}$  M in (see Fig S9 at different concentrations in methanol) and the excitation wavelengths is 273 nm.

As summary, relatively large metal-organic nanocapsules can be self-assembled by using carboxylic-heptazine ligands. The presence of the  $C_6N_7$  heptazine moiety in the ligand opens wide possibilities to combine its photochemical and catalytic properties with those of the metals. Furthermore, this is an example of how to circumvent the problems to synthesize complex systems with low-solubility ligands.

## ASSOCIATED CONTENT

The Supporting Information is available free of charge at

Details of synthesis and characterization (IR data, NMR, mass spectrometry, AFM), DFT calculations and crystallographic data, CCDC-1951192 contains the supplementary crystallographic data for trinuclear complex. These data can be obtained free of charge via <http://www.ccdc.cam.ac.uk/conts/retrieving.html> or from the Cambridge Crystallographic Data Centre, 12 Union Road, Cambridge CB2 1EZ, UK; fax: +44 (0) 1223-336-033; or e-mail: [deposit@ccdc.cam.ac.uk](mailto:deposit@ccdc.cam.ac.uk).



## ACKNOWLEDGEMENTS

This work had Financial Support by the Ministerio de Ciencia e Innovación through grant PGC2018-093863-B-C21 and MDM-2017-0767 and Generalitat de Catalunya with the grant SGR2017-1289. E.R. thanks Generalitat de Catalunya for his ICREA Academia grant. L.M. thanks Conicyt-Chile for a predoctoral fellowship. S. G.-C. thanks Generalitat de Catalunya for a Beatriu de Pinós Fellowship (2017 BP 00080). We thank the CSUC for computational resources. Characterization of the samples were carried out in the CCiTUB (Centres Científics i Tecnològics de la Universitat de Barcelona).

## REFERENCES

- (1) Kaphan, D. M.; Levin, M. D.; Bergman, R. G.; Raymond, K. N.; Toste, F. D., A supramolecular microenvironment strategy for transition metal catalysis. *Science* **2015**, *350*, 1235-1238.
- (2) Dai, F.-R.; Sambasivam, U.; Hammerstrom, A. J.; Wang, Z., Synthetic Supercontainers Exhibit Distinct Solution versus Solid State Guest-Binding Behavior. *J. Am. Chem. Soc.* **2014**, *136*, 7480-7491.
- (3) Cook, T. R.; Stang, P. J., Recent Developments in the Preparation and Chemistry of Metallacycles and Metallacages via Coordination. *Chem. Rev.* **2015**, *115*, 7001-7045.
- (4) Caulder, D. L.; Raymond, K. N., Supermolecules by design. *Acc. Chem. Res.* **1999**, *32*, 975-982.
- (5) Byrne, K.; Zubair, M.; Zhu, N.; Zhou, X.-P.; Fox, D. S.; Zhang, H.; Twamley, B.; Lennox, M. J.; Duren, T.; Schmitt, W., Ultra-large supramolecular coordination cages composed of endohedral Archimedean and Platonic bodies. *Nat. Commun.* **2017**, *8*, 15268.
- (6) Brown, C. J.; Toste, F. D.; Bergman, R. G.; Raymond, K. N., Supramolecular Catalysis in Metal-Ligand Cluster Hosts. *Chem. Rev.* **2015**, *115*, 3012-3035.
- (7) Pluth, M. D.; Raymond, K. N., Reversible guest exchange mechanisms in supramolecular host-guest assemblies. *Chem. Soc. Rev.* **2007**, *36*, 161-171.

- (8) Pasquale, S.; Sattin, S.; Escudero-Adan, E. C.; Martinez-Belmonte, M.; de Mendoza, J., Giant regular polyhedra from calixarene carboxylates and uranyl. *Nat. Commun.* **2012**, *3*, 785.
- (9) Zhang, D. W.; Ronson, T. K.; Nitschke, J. R., Functional Capsules via Subcomponent Self-Assembly. *Acc. Chem. Res.* **2018**, *51*, 2423-2436.
- (10) Zarra, S.; Wood, D. M.; Roberts, D. A.; Nitschke, J. R., Molecular containers in complex chemical systems. *Chem. Soc. Rev.* **2015**, *44*, 419-432.
- (11) Roberts, D. A.; Pilgrim, B. S.; Nitschke, J. R., Covalent post-assembly modification in metallosupramolecular chemistry. *Chem. Soc. Rev.* **2018**, *47*, 626-644.
- (12) Wu, K.; Li, K.; Hou, Y.-J.; Pan, M.; Zhang, L.-Y.; Chen, L.; Su, C.-Y., Homochiral D<sub>4</sub>-symmetric metal-organic cages from stereogenic Ru(II) metalloligands for effective enantioseparation of atropisomeric molecules. *Nat. Commun.* **2016**, *7*, 10487.
- (13) Yeung, C.-T.; Yim, K.-H.; Wong, H.-Y.; Pal, R.; Lo, W.-S.; Yan, S.-C.; Wong, M. Y.-M.; Yufit, D.; Smiles, D. E.; McCormick, L. J.; Teat, S. J.; Shuh, D. K.; Wong, W.-T.; Law, G.-L., Chiral transcription in self-assembled tetrahedral Eu<sub>4</sub>L<sub>6</sub> chiral cages displaying sizable circularly polarized luminescence. *Nat. Commun.* **2017**, *8*, 1128.
- (14) Zhang, T.; Zhou, L.-P.; Guo, X.-Q.; Cai, L.-X.; Sun, Q.-F., Adaptive self-assembly and induced-fit transformations of anion-binding metal-organic macrocycles. *Nat. Commun.* **2017**, *8*, 15898.
- (15) Liebig, J., Ueber einige Stickstoff-Verbindungen. *Ann. Pharm.* **1834**, *10*, 1-47.
- (16) Zhao, Z. W.; Sun, Y. J.; Dong, F., Graphitic carbon nitride based nanocomposites: a review. *Nanoscale* **2015**, *7*, 15-37.
- (17) Wang, Y.; Wang, X. C.; Antonietti, M., Polymeric Graphitic Carbon Nitride as a Heterogeneous Organocatalyst: From Photochemistry to Multipurpose Catalysis to Sustainable Chemistry. *Angew. Chem. Inter. Ed.* **2012**, *51*, 68-89.
- (18) Ong, W. J.; Tan, L. L.; Ng, Y. H.; Yong, S. T.; Chai, S. P., Graphitic Carbon Nitride (g-C<sub>3</sub>N<sub>4</sub>)-Based Photocatalysts for Artificial Photosynthesis and Environmental Remediation: Are We a Step Closer To Achieving Sustainability? *Chem. Rev.* **2016**, *116*, 7159-7329.
- (19) Cao, S. W.; Low, J. X.; Yu, J. G.; Jaroniec, M., Polymeric Photocatalysts Based on Graphitic Carbon Nitride. *Adv. Mater.* **2015**, *27*, 2150-2176.

- (20) Zhao, X.; He, H.; Hu, T.; Dai, F.; Sun, D., Interpenetrating Polyhedral MOF with a Primitive Cubic Network Based on Supramolecular Building Blocks Constructed of a Semirigid C<sub>3</sub>-Symmetric Carboxylate Ligand. *Inorg. Chem.* **2009**, *48*, 8057-8059.
- (21) Maxwell, L.; Gómez-Coca, S.; Weyhermüller, T.; Panyella, D.; Ruiz, E., A trinuclear CuII complex with functionalized s-heptazine N-ligands: molecular chemistry from a g-C<sub>3</sub>N<sub>4</sub> fragment. *Dalton Trans.* **2015**, *44*, 15761-15763.